PENSOFT.

SENCKENBERG
world of biodiversity

Leibniz
Association

A morphometric approach to the comparative morphology of aedeagi shapes in net-winged beetles: A case study on the *Macrolycus dotatus* species group (Coleoptera: Lycidae)

Hao Yu Liu[1], Ruo Lan Du[1], Wei Zhao[1], Xing Ke Yang[2], Yu Xia Yang[1]

1 *Key Laboratory of Zoological Systematics and Application, School of Life Science, Institute of Life Science and Green Development, Hebei University, Baoding 071002, China*

2 *Key Laboratory of Zoological Systematics and Evolution, Institute of Zoology, Chinese Academy of Sciences, Beijing, China*

https://zoobank.org/39E0B43B-FFBD-46BF-BA86-F79314C7BE34

Corresponding authors: Hao Yu Liu (liuhy@hbu.edu.cn), Yu Xia Yang (yxyang@hbu.edu.cn)

Citation: Liu HY, Du RL, Zhao W, Yang XK, Yang YX (2023) A morphometric approach to the comparative morphology of aedeagi shapes in net-winged beetles: A case study on the *Macrolycus dotatus* species group (Coleoptera, Lycidae). Arthropod Systematics & Phylogeny 81: 897–916. https://doi.org/10.3897/asp.81.e111281

Abstract

Insect male genitalia show an evolutionarily variable morphology that is valuable for both species identification and phylogenetic analyses. However, we often encounter some difficulties when conducting relevant studies due to only quantitative variations exhibited in male genitalia. In this study, based on the taxonomy of the *Macrolycus dotatus* species group (a total of seven species, including three new species described here), we analyzed the male genitalia shapes by GM and then constructed the phenotypic relationships by UPGMA, NJ and MP analyses. The results demonstrated that the species could be well delineated by the shape of male genitalia, and the produced phenograms frequently recovered phenotypic similarity between the coupled species, including *M. atronotatimimus* **sp. nov.** + *M. huoditangensis* **sp. nov.** and *M. aemulus* + *M. dotatus*, which is useful for making comparisons in species descriptions. Meanwhile, the MP analysis of male genitalia shape using two landmark configurations is considered reliable in inferring the phylogenetic relationship among species in terms of the consistency between its topologies and the molecular phylogeny. This study sheds new light on improving the morphological taxonomy of insects in lower grades while fully utilizing the taxonomic value of male genitalia in a phylogenetic context.

Key words

Geometric morphometrics, phylogenetic morphometrics, taxonomy, new species, net-winged beetles

1. Introduction

As animals with internal fertilization, numerous insect species have species-specific male genitalia with morphological divergence among closely related species (Eberhard 1985). Insect male genitalia are among the most evolutionarily variable morphological features, and their apparently fast rate of morphological change has been hypothesized to be due to sexual selection (e.g., Simmons 2014). They provide systematists with diagnostic features at various taxonomic levels (Schuh and Slater, 1995). In particular, they have been considered one of the

most important and useful specific diagnostic characteristics in insect systematics (Tuxen 1970).

While often used as species diagnostic characters, insect male genitalia are also proven to be valuable in phylogenetic analyses (Yoshizawa and Johnson 2006). They normally serve in classifications and phylogenetic frameworks at higher taxonomic hierarchical levels, e.g., in Cantharidae at the subfamilial level (Brancucci 1980) and Lycidae at least at the tribal level (Bocak and Bocakova 1990, 2008). However, in the lower grades, the phylogenetic value of male genitalia has been rarely studied. This is probably because the differences in male genitalia are usually subtle within a genus, exhibiting quite uniform structures but showing quantitative differences in shapes. This resulted in some difficulties in evaluating the relationship among the species based on male genitalia, although they are highly valued in the systematics, thereby hardly recognizing its sibling species to make comparisons when describing a new species. Such conditions are common in insects, but few studies have been conducted to quantify such male genitalia variations for phylogenetic reconstruction. The advent of geometric morphometrics (GM) and phylogenetic morphometrics (PM) methods make it possible for us to investigate the phylogenetic relationships to the specific level based on the shapes of male genitalia.

Geometric morphometrics offers a more comprehensive and effective approach to the study of shape through the multivariate statistical analysis of anatomical landmarks or outlines of biological homology (Bookstein 1991; Rohlf and Marcus 1993; Adams et al. 2004). It preserves information about the relative spatial arrangement of the data through analysis (Zelditch et al. 2004), making it possible to find and analyze shape variations in organisms within and between populations (Walker 2000). Furthermore, it is considered to be the most rigorous morphometric method (Gilchrist et al. 2000; Debat et al. 2003). Moreover, geometric morphometric tools present the advantage of laying results that not only have high statistical power but also have easily visualized results, helping with their interpretation and communication (Rohlf and Marcus 1993; Adams et al. 2004; Zelditch et al. 2004). It has been successfully used to resolve taxonomic uncertainties and in delineating cryptic species of several insect groups (i.e., Matias et al. 2001; De la Riva et al. 2001; Villegas et al. 2002; Baylac et al. 2003; Dujardin et al. 2003; Roggero and Dentrèves 2005; Aytekin et al. 2007; Sadeghi et al. 2009; Francuski et al. 2009; Tüzün 2009; Faille et al. 2007; Hájek and Fikáček 2010; Xu et al. 2013; Li et al. 2016), mostly by analyzing the shapes of the wing and a few of the pronotum and male genitalia. Additionally, geometric morphometrics can be used to determine shape differences, and the resulting phenograms can effectively indicate phenetic relationships between the samples, summarizing overall patterns of similarity (Pretorius and Scholtz 2001). In particular, with the arrival of the phylogenetic morphometric (PM) analysis method (Díaz-Cruz et al. 2021), we could explore the relationships among organisms based on morphometric data. Most recently, wing shapes have been

proven valuable in inferring phylogenetic proximity at the generic level (Zhao et al. 2023). However, no study has been conducted to evaluate the significance of male genitalia shapes in assessing the phylogenetic relationship at the specific level until now.

Lycidae (commonly known as net-winged beetles) is a moderately large group within Elaterodea that currently encompasses approximately 4600 described species (Masek et al. 2018) yet exhibits an astounding diversity of male genitalic structures. Structural variation at least across the tribes or genera has been recognized (Bocak and Bocakova 1990, 2008). For example, in Macrolycini (including the sole member of *Macrolycus* Waterhouse, 1878), the male genitalia has a simple and uniformly hooded basal piece, a slender and highly sclerotized median lobe that is more or less globally inflated at the subapical part bearing an oval ventral cavity, and a simple, slender and membranous internal sac with its most apical part exposed (Bocak and Bocakova 1990; Li et al. 2012). The lateral lobes are present (subgenus *Macrolycus*) or absent (subgenus *Cerceros* Kraatz, 1879) to separate this genus into two subgenera, which are further divided into nine species groups (Li et al. 2015). Within each species group, each component of the male genitalia is consistent among the species, exhibiting some quantitative variations in the shapes of the median lobe, plus its high sclerotization, which makes them methodologically advantageous for GM analysis. Therefore, the species group *Macrolycus* is thought to be an ideal candidate taxon to conduct GM and PM analyses of male genitalia shapes.

In the present study, taking the *Macrolycus dotatus* species group (a total of seven species, including the new species described here) as an example, we will analyze the shape of male genitalia of the species by GM, assess phenetic relationships based on these morphometric data, and then explore the phylogenetic relationships by PM. Based on these results, we are going to describe the male genitalia with the morphometric data, and to recognize the similar or sibling species to make comparison with the new species, which is a necessary content for the new species description in the modern taxonomy. This study will shed new light on the morphological taxonomy of insects in lower grades while fully utilizing the taxonomic value of the male genitalia; in particular, it will provide some inspiration to obtain a more dependable phylogeny among those taxa if unavailable with molecular data.

2. Material and methods

2.1. Studied material

The studied material of the *M. dotatus* species group is preserved at the Institute of Zoology, Chinese Academy of Sciences, Beijing, China (IZAS) and the Museum of Hebei University, Baoding, China (MHBU).

2.2. Taxonomic study

We identified the species of the *M. dotatus* species group by relevant references (Kazantsev 1993; Li et al. 2012, 2015; Li 2015). The description format and terminology follow those of Li et al. (2012). Additionally, the male genitalia shape will be included in the description for the first time. In addition, the similar species in the male genitalia shapes shall be compared with the new species in discussing the parallax discrimination.

2.3. Photography and measurements

The specimens were softened in water, and the male genitalia were dissected, cleared in 10% NaOH solution, examined and photographed in glycerol, and finally glued on a paper card for permanent preservation. Images of adults were taken with a Canon EOS 80D digital camera and aedeagi by a Leica M205A stereomicroscope and then stacked in Helicon Focus 7. The final permutation was edited in Adobe Photoshop CS3.10.0.1. The measurements were taken with ImageJ 1.50i (NIH, USA). Body length was measured from the anterior margin of the head to the elytral apex, and the width was measured across the humeral part of the elytra. Pronotal length was measured from the middle of the anterior margin to the middle of the posterior margin and the width across the widest part of the pronotum. Eye diameter was measured at the widest point, and the interocular distance was taken at the point of minimum.

2.4. Geometric data acquisition and digitalization

All of the species of the *M. dotatus* species group were included in the analysis. Digital photographs of male genitalia were annotated using TpsUtil 1.43 software (Rohlf 2008a, see http://life2.bio.sunysb.edu/morph). Two curves were extracted from the ventral and lateral contours of the median lobe to represent the external forms. The ventral cavity is neglected in the analysis due to its
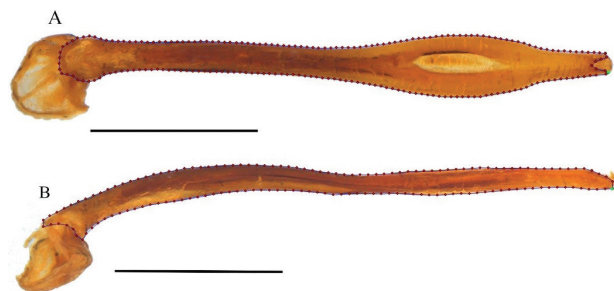

Figure 1. Description of the curves used in the geometric morphometric analysis, represented by *Macrolycus atronotatus* Pic, 1939. Curves were resampled into 200 semilandmarks for the contours of the median lobe of the aedeagus in (**A**) ventral and (**B**) lateral views. The semilandmarks of the start and terminal ones are shown in green points. Scale bars: 1.0 mm.

variation within some species (Li et al. 2012). The two curves both started from apices and ended at the same point and were resampled into 200 equally spaced semilandmarks (Fig. 1A, B). All curves and semilandmarks were digitized with TpsDig 2.12 software (Rohlf 2008b, see http://life2.bio.sunysb.edu/morph). The digitalization procedure was repeated three times by the same observer on different days to evaluate landmark measurement error (Zhao et al. 2023).

Then, we used TpsSmall (ver. 1.20, F. Rohlf, see http://life2.bio.sunysb.edu/ morph) to test whether the observed variation in shape was sufficiently small that the distribution of points in the tangent space could be used as a good approximation of the distribution in shape space. The coordinates were analyzed using TpsRelw (ver. 1.49, F. Rohlf, see http://life2.bio.sunysb.edu/morph) to calculate eigenvalues for each principal warp. The shape changes of different species implied by variation along the first two relative warp axes and shape changes were shown as transformation grids using thin-plate splines.

2.5. Geometric morphometric (GM) analyses

To examine shape variation, the digitized outline data were analyzed using MorphoJ 1.06d software (Klingenberg 2011, see http://life2.bio.sunysb.edu/morph). Principal component analysis (PCA) was employed to test how well the species could be distinguished by the shape of the median lobe. Frequently, the characters with high loading values in PCAs correspond to the observed variation patterns among species. The relative similarity and discrimination of the test groups was analyzed using canonical variates analysis (CVA). CVA finds shape values that maximize group means relative to variation within groups by assuming that covariate matrices are identical (Klingenberg 2010). Mahalanobis and Procrustes distances (the square root of the sum of squared differences between corresponding points) between the species were computed, and the matrix was produced by MorphoJ software (Klingenberg 2011).

2.6. Phylogenetic morphometric (PM) analyses

The phylogenetic relationships among the species were based on the morphometric data of male genitalia considering UPGMA (unweighted pair group method using arithmetic averages), neighbor-joining (NJ) and maximum parsimony (MP) as the optimality criteria (Champakaew et al. 2021; Goloboff and Catalano 2016). Procrustes and Mahalanobis distance matrices were subjected to UPGMA and cluster analyses to determine the phenetic relationships among the species. In addition, neighbor-joining (NJ) trees (Sneath and Sokal 1973) were constructed to display the Mahalanobis and Procrustes distances between populations using PAST 2.17 with 1000 bootstrap replicates.

The tps files produced in tps-DIG were also used to perform MP analysis in TNT 1.5 (Goloboff and Catalano 2016). The search strategy followed a heuristic (traditional search) using random addition sequences and tree bisection reconnection (TBR) as the branch swapping algorithm, holding one tree per replicate and 1000 runs (mult = ras tbr hold 1 rep 1000) (Díaz-Cruz et al. 2021).

2.7 Preparation of distribution map

The distribution information was collected from the Global Biodiversity Information Facility (GBIF, https://www.gbif.org), relevant publications (Pic 1923, 1935, 1939; Kleine 1925, 1933, 1942; Nakane 1967, 1969; Kazantsev 1993, 2001, 2002, 2011; Li et al. 2012, 2015) and our material in the present study. The distribution map was prepared using ArcMap 10.8 and edited in Adobe Photoshop CS3.10.0.1.

3. Results

3.1 Taxonomy

Macrolycus dotatus species group

Diagnosis. The *M. dotatus* species group is attributed to the subgenus *Cerceros* because of its absence of lateral lobes in male genitalia, and it differs from other species groups by the characteristic shape of the apex of the median lobe, which bears a ventrally curved process (Li et al. 2015).

Included species. *M. atronotatus* Pic, 1939, *M. jianfenglingensis* Li, Bocak & Pang, 2015, *M. dotatus* Kleine, 1925, *M. aemulus* Barovskij, 1930, *M. unicolor* Y. Yang, Liu & X. Yang, **sp. nov.**, *M. huoditangensis* Y. Yang, Liu & X. Yang, **sp. nov.** and *M. atronotatimimus* Y. Yang, Liu & X. Yang, **sp. nov.**

Distribution (Fig. 2). China (Yunnan, Shaanxi, Anhui, Hainan, Guangxi, Guangdong, Sichuan, Jilin, Heilongjiang, Liaoning), Vietnam, Laos, Japan, South Korea, Russia (Far East).

Macrolycus atronotatus Pic, 1939

Figures 3A, 4A–C, 5A, 8A, B

Macrolycus atronotatus Pic, 1939: 165; Kleine, 1942: 21; Kazantsev, 1993: 50; 2001: 100; Li et al., 2012: 48.

Material examined. China • 1♂ (IZAS); Sichuan, Emei Mt.; 2100–3100 m; 25.VI.1955; X. C. Yang leg.

Descriptive notes. Male (Fig. 3A). Antennae (Fig. 5A) flabellate, overlapping two-thirds the length of the elytra when inclined. Antennomere II transverse; III–XI lamellate, lamella of antennomere III 1.2 times as long as joint itself, and lamella of VIII longest, 3.9 times longer than joint itself. — **Aedeagus:** median lobe nearly in a
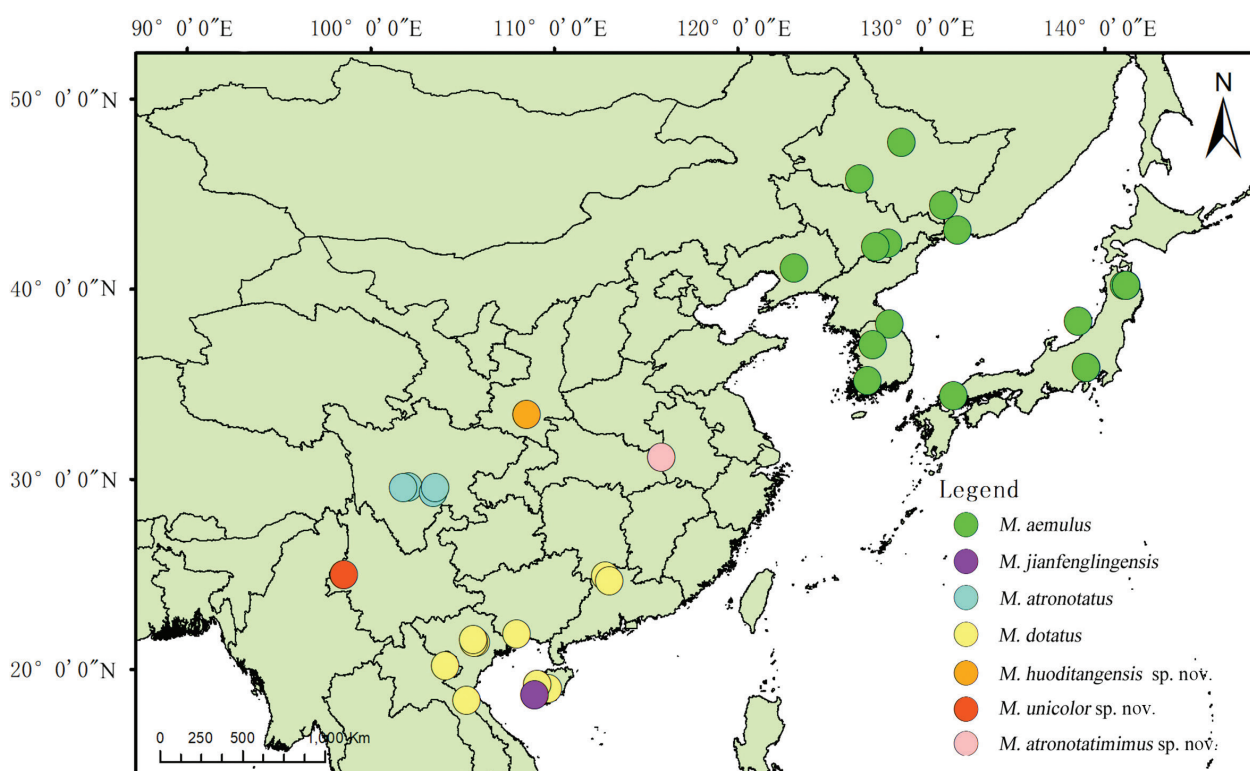

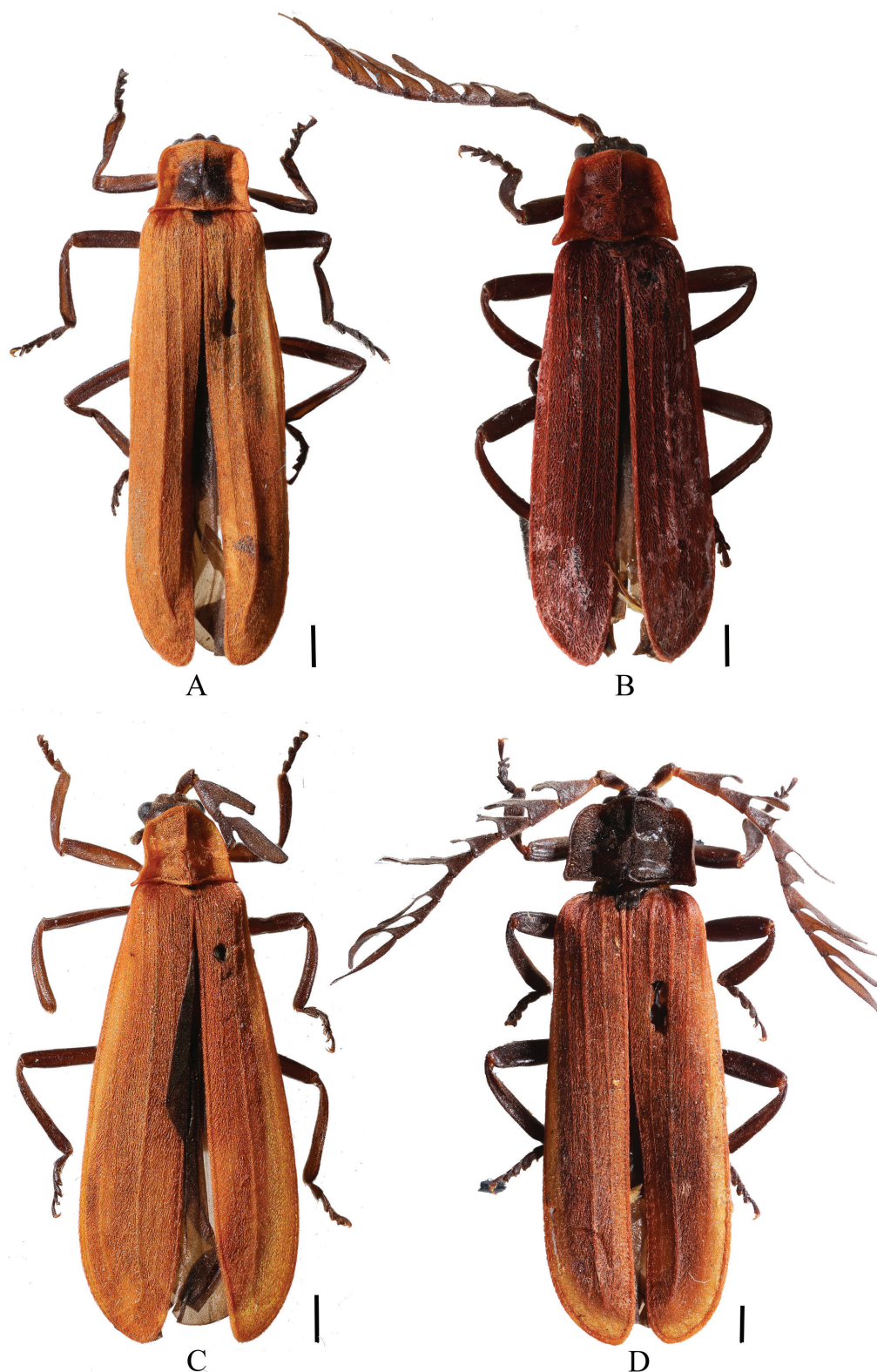**Figure 2.** Distribution map of the *Macrolycus dotatus* species group in the world.

Figure 3. Male habitus of *Macrolycus* species, dorsal views: **A** *M. atronotatus* Pic, 1939; **B** *M. jianfenglingensis* Li, Bocak & Pang, 2015; **C** *M. dotatus* Kleine, 1925; **D** *M. aemulus* Barovskij, 1930. Scale bars: 1.0 mm.

horizontal line between basal and apical parts on dorsal side in lateral view (Figs 4C, 8A); almost parallel-sided at basal part in dorsal (Fig. 4A) and ventral (Figs 4B, 8B) views, subapical part inflated laterally not dorsally (Fig. 4C), ventral cavity narrowly fusiform, apical part gradually narrowed distad, with a deep U-shaped notch at apex (Fig. 4C).

Distribution. China (Sichuan, Shaanxi).

Remarks. The type locality is "Chansi" (Pic 1939), which is inaccurate. Additionally, there is no additional record from Shaanxi in later studies (Kleine 1942; Kazantsev 1993, 2001; Li et al. 2012). Thus, only the records from Sichuan are present in the distribution map herein.
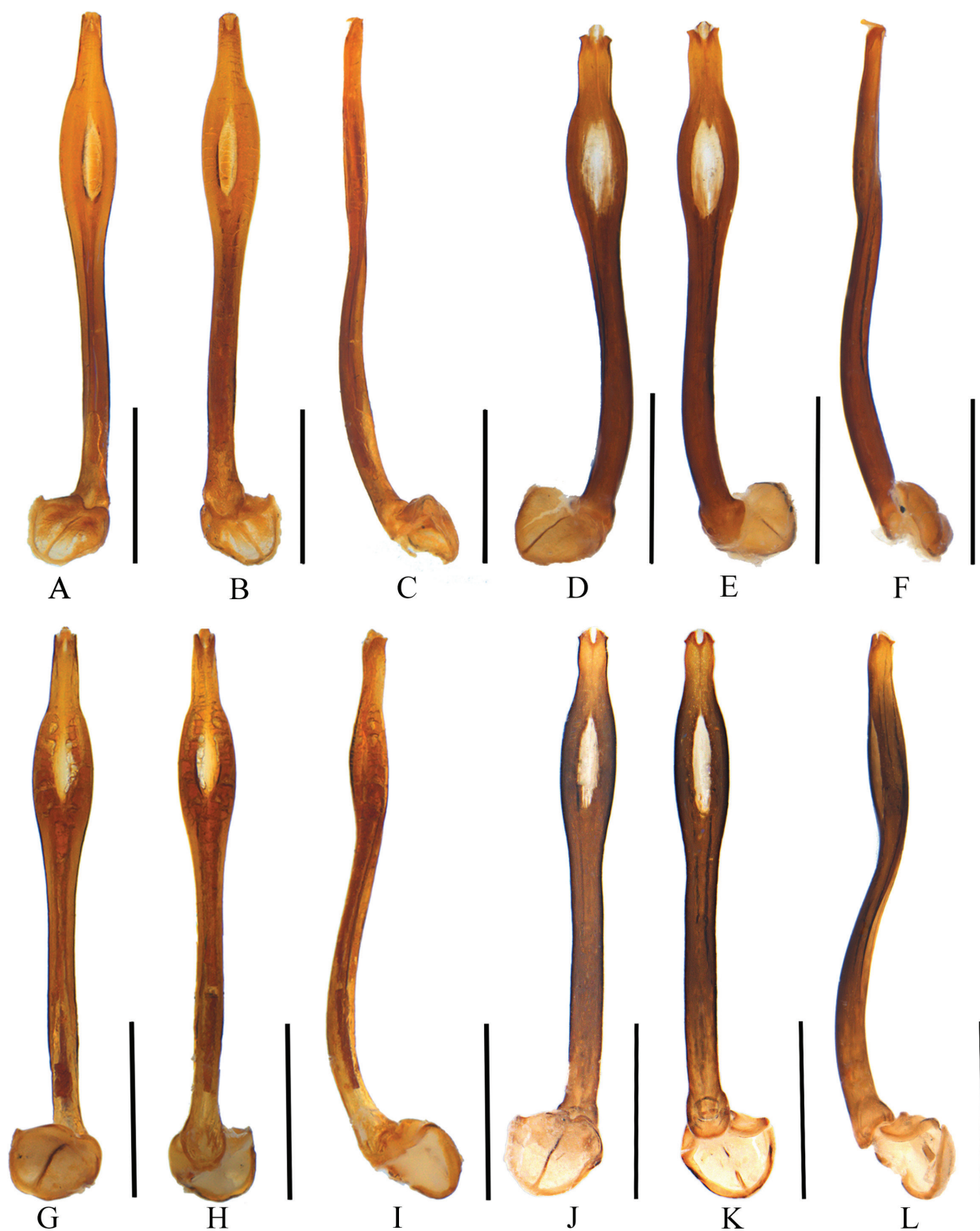
Figure 4. Aedeagi of *Macrolycus* species: **A–C** *M. atronotatus* Pic, 1939; **D–F** *M. jianfenglingensis* Li, Bocak & Pang, 2015; **G–I** *M. dotatus* Kleine, 1925; **J–L** *M. atronotatimimus* **sp. nov.** A, D, G, J: dorsal views; B, E, H, K: ventral views; C, F, I, L: lateral views. Scale bars: 1.0 mm.

Macrolycus jianfenglingensis Li, Bocak & Pang, 2015

Figures 3B, 4D–F, 5B, 8A, B

Macrolycus jianfenglingensis Li, Bocak & Pang, 2015:325, Figs 7, 24, 25, 43.

Material examined. China • 2♂ (IZAS); Hainan, Jianfengling; 1984; G. Q. Mai leg.

Descriptive notes. Male (Fig. 3B). Antennae (Fig. 5B) flabellate, overlapping two-thirds the length of the elytra when inclined. Antennomere II transverse; III–XI lamellate, lamella of antennomere III 0.8 times as long as joint

Figure 5. Right antennae of *Macrolycus* species, dorsal views: **A** *M. atronotatus* Pic, 1939; **B** *M. jianfenglingensis* Li, Bocak & Pang, 2015; C. *M. dotatus* Kleine, 1925; **D** *M. aemulus* Barovskij, 1930; **E** *M. unicolor* **sp. nov.**; **F** *M. huoditangensis* **sp. nov.**; **G** *M. atronotatimimus* **sp. nov.** Scale bars: 1.0 mm.

itself, and lamella of IX longest, 5.1 times longer than joint itself. — **Aedeagus:** median lobe nearly in a horizontal line between basal and apical parts on dorsal side in lateral view (Figs 4F, 8A); obviously curved at base in dorsal (Fig. 4D) and ventral (Figs 4E, 8B) views, subapical part inflated laterally and feebly inflated dorsally (Fig. 4F), ventral cavity nearly oblong, apical part nearly parallel-sided, slightly sinuate before apices, with a deep V-shaped notch at apex (Fig. 4D).

Distribution. China (Hainan).

Remarks. We have provided a detailed description of the characteristics of antennomere III and male genitalia here.

Macrolycus dotatus Kleine, 1925

Figures 3C, 4G–I, 5C, 8A, B

Macrolycus dotatus Kleine, 1925: 328; 1933: 5; Nakane, 1967: 73; Li et al., 2012: 49.

Material examined. China • 1♂ (IZAS); Yunnan, Simao; 13.IV.1955; Y. Z. Zi leg.; 1♀ (IZAS); same locality; 13.IV.1955; Y. Z. Zi leg.

Descriptive notes. Male (Fig. 3C). Antennae (Fig. 5C) flabellate, overlapping two-thirds the length of the elytra when inclined. Antennomere II transverse; III–XI lamellate, antennomere III with lamella nearly as long as joint, and lamella of IX longest, 5.0 times longer than joint itself. — **Aedeagus:** median lobe moderately curved near

middle in lateral view, at an angle of ca. 150° between basal and apical parts of dorsal side, distinctly arcuate at base part, subapical part moderately inflated dorsally (Figs 4I, 8A); nearly straight at basal part in ventral view, subapical part strongly inflated laterally (Figs 4H, 8B), with a fusiform ventral-cavity (Fig. 4H); apical part gradually narrowed distad, with a deep V-shaped notch at apex (Fig. 4G).

Distribution. China (Hainan, Guangxi, Guangdong, Yunnan), Vietnam, Laos.

Remarks. In the latest work (Li et al. 2012), this species was not illustrated. Here, we provide illustrations of the male habitus, antenna and aedeagus to make it better known.

Macrolycus aemulus Barovskij, 1930

Figures 3D, 5D, 7A–E, 8A, B

Macrolycus aemulus Barovskij, 1930: 580; Kleine, 1933: 5; 1942: 20; Pic, 1935: 115; Nakane, 1967: 73; 1969: 33; Kazantsev, 2001: 100; 2011: 390.

Macrolycus kleinei Nakane, 1967: 71. Synonymized by Nakane, 1969: 33.

Macrolycus flabellatus var. *laticollis* Pic, 1935: 110. Synonymized by Nakane, 1969: 33.

Material examined. China • 1♀(MHBU); Liaoning, Anshan, Qianshan; 7.VII.2012; Z. X. Zhang & L. F. Wang leg.; 1♂(MHBU); Heilongjiang, Suifenhe; 15.VII.2003;

X. J. Yang & S. S. Liu leg.; 3♂2♀ (IZAS); Heilongjiang, Haerbin; 6.VI.1954; collector unknown; 1♀ (IZAS); Heilongjiang, Yichun; 4.VIII.1956; collector unknown; 2♂ (IZAS); Jilin, Fusong; 21.VI.1955; collector unknown; 1♂ 1♀(IZAS); Jilin, Changbaishan; 1200 m; G. Y. Deng leg.; 2♀ (IZAS); Jilin, Changbaishan; 6.VII.1985; collector unknown.

Descriptive notes. Male (Fig. 3D). Antennae (Fig. 5D) flabellate, overlapping half-length of elytra when inclined. Antennomere II transverse; III–XI lamellate, antennomere III with lamella nearly as long as joint itself, and lamella of IX longest, 3.2 times longer than joint itself. — **Aedeagus:** median lobe moderately curved near middle in lateral view, at an angle of ca. 150° between basal and apical parts of dorsal side, moderately arcuate at base part, subapical part slightly inflated dorsally (Figs 7C, 8A); moderately curved at basal part in ventral view, subapical part moderately inflated laterally (Figs 7B, 8B), with a fusiform ventral cavity (Fig. 7B); apical part gradually narrowed distad (Fig. 7A, B, D), with a deep V-shaped notch at apex (Fig. 7A, D).

Remark. In terms of the special structure at the apex of the median lobe (Fig. 7D, E), we suggest placing this species into the *M. dotatus* species group.

Distribution. China (Jilin, Heilongjiang, Liaoning), Japan, South Korea, Russia.

Macrolycus unicolor Y. Yang, Liu & X. Yang, sp. nov.

https://zoobank.org/18F1806E-B5A1-481F-B34A-C7F-C9A68048B

Figures 5E, 6B, 7F–H, 8A, B

Type material. Holotype: China • ♂ (IZAS); Yunnan, Tengchong; 20.V.2006; H.B. Liang leg.

Description. Male (Fig. 6B). Length 8.2 mm, width at humeri 1.7 mm. — Body brown. Pronotum, elytra and scutellum orange. Surface covered with decumbent orange pubescence. — Head relatively small. Eyes small, interocular distance approximately twice as large as eye diameter. Antennae (Fig. 5E) flabellate, overlapping two-thirds the length of the elytra when inclined. Antennomere II transverse; III–XI lamellate, lamella of III 0.8 times as long as the joint itself, and lamella of VIII longest, 4.0 times longer than the joint itself. — Pronotum quadrate, 1.14 times wider than long, disc present with a median longitudinal keel extending from anterior margin to middle part. Anterior margin approximately straight, lateral margins subparallel and posterior margin bisinuate; anterior angles obtuse, posterior angles sharp and prominently projected. Scutellum trapezoidal, feebly emarginate at apex. — Elytra slender and subparallel, 3.2 times longer than humeral width. Each elytron with four

costae, costa II stronger than the others; costa III visible only at basal part. — **Aedeagus:** median lobe slender, strongly curved near middle in lateral view, at an angle of ca. 120° between basal and apical parts of dorsal side, strongly arcuate at base part, subapical part strongly inflated dorsally (Figs 7H, 8A); naerly straight at basal part in ventral view, subapical part strongly inflated laterally and asymmetrical (Figs 7F, G; 8B), with an oval ventral cavity (Fig. 7G); apical part parallel-sided (Fig. 7F, G), with a deep V-shaped notch at apex (Fig. 7G).

Female. Unknown.

Diagnosis. This new species resembles *M. atronotatus* in appearance but differs from the latter in the uniformly orange pronotum (Fig. 6B), with a black patch on the pronotum (Fig. 3A) in *M. atronotatus*. Additionally, it is similar to *M. atronotatimimus* **sp. nov.** in the lateral view of the median lobe (Fig. 8A) but differs from the latter in the ventral view (Fig. 8B), which is feebly curved at the basal part, at an angle of ca. 15° with the apical part, with the subapical part asymmetrically inflated (Fig. 7G). In comparison, the median lobe of *M. atronotatimimus* **sp. nov.** is moderately swollen and straight at the basal part in ventral view (Fig. 4K).

Etymology. The specific name is derived from the Latin "*uni-*" (single) and "*color*" (hue), referring to its uniformly orange pronotum.

Distribution. China (Yunnan).

Macrolycus huoditangensis Y. Yang, Liu & X. Yang, sp. nov.

https://zoobank.org/41B6DD63-BFC8-49B1-875E-76E59A5534DB

Figures 5F, 6C, 7I–K, 8A, B

Type material. Holotype: China • ♂ (IZAS); Shaanxi, Ningshan, Huoditang Forestry; 2.VI.2007; M. Y. Lin. leg.

Description. Male (Fig. 6C). Length 8.0 mm, width at humeri 1.8 mm. — Body brown to black. Pronotum, elytra and scutellum dark red. Surface covered with decumbent red pubescence. — Head relatively small. Eyes small, interocular distance approximately twice as large as eye diameter. Antennae (Fig. 5F) flabellate, overlapping half-length of elytra when inclined. Antennomere II transverse; III–XI lamellate, lamella of III 1.1 times longer than joint itself; lamella of VII longest, 4.5 times longer than joint itself.

Pronotum trapezoidal, 1.3 times wider than long, disc present with a median longitudinal keel extending from anterior margin to middle part. Anterior margin weakly convex and forms a small pointed process, lateral margins sinuate and posterior margin straight; anterior angles confluent with anterior margin, posterior angles

posterior angles sharp and prominently projected. Scutellum trapezoidal, straight at apex. — Elytra slender and subparallel, 4.0 times longer than humeral width. Each elytron had four costae, costae I, II and IV, which were stronger than costa III. — **Aedeagus:** median lobe stout, strongly curved near middle in lateral view, at an angle
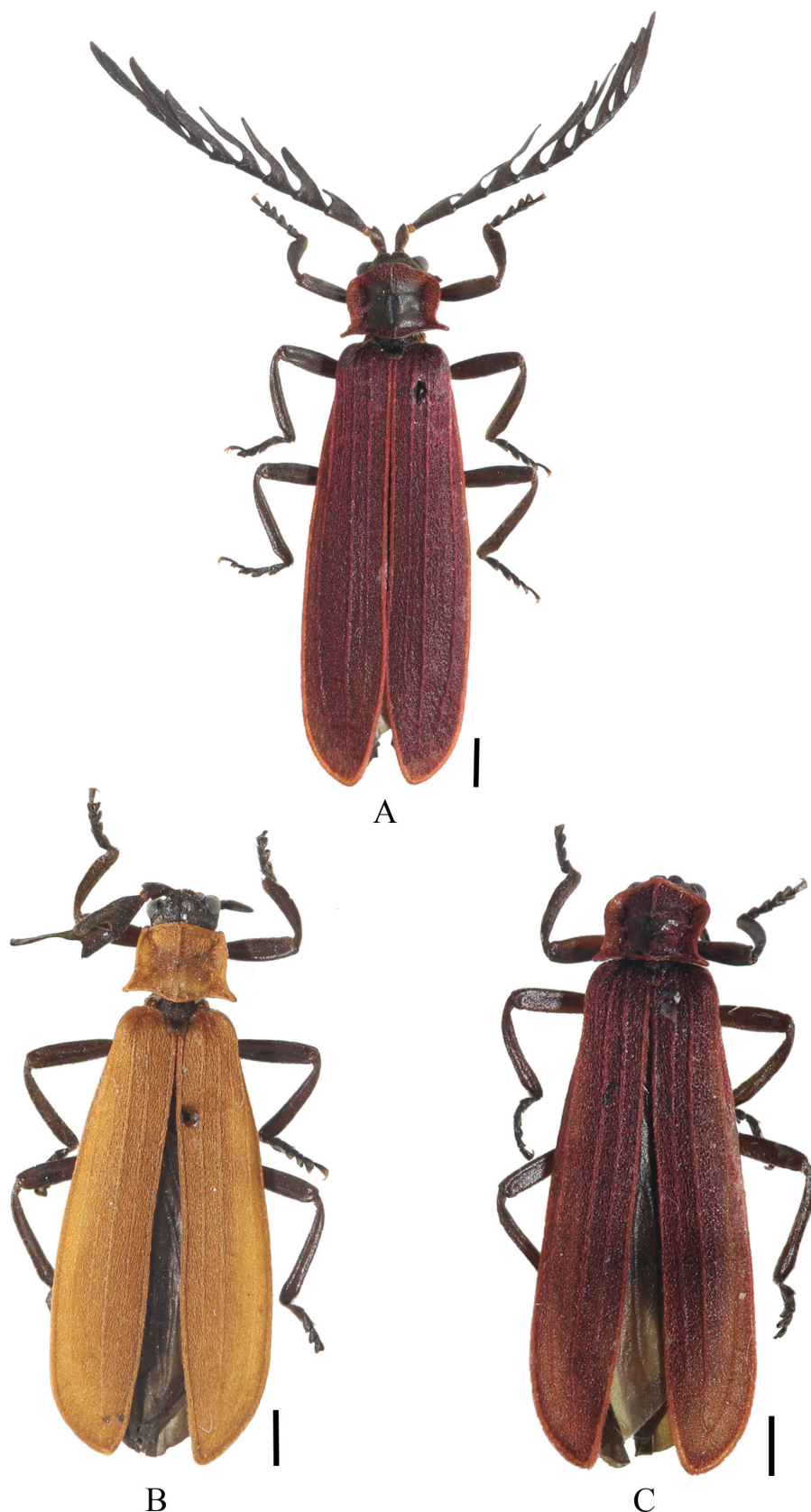

Figure 6. Holotype male habitus of *Macrolycus* species, dorsal views: **A** *M. atronotatimimus* **sp. nov.**; **B** *M. unicolor* **sp. nov.**; **C** *M. huoditangensis* **sp. nov.** Scale bars: 1.0 mm.
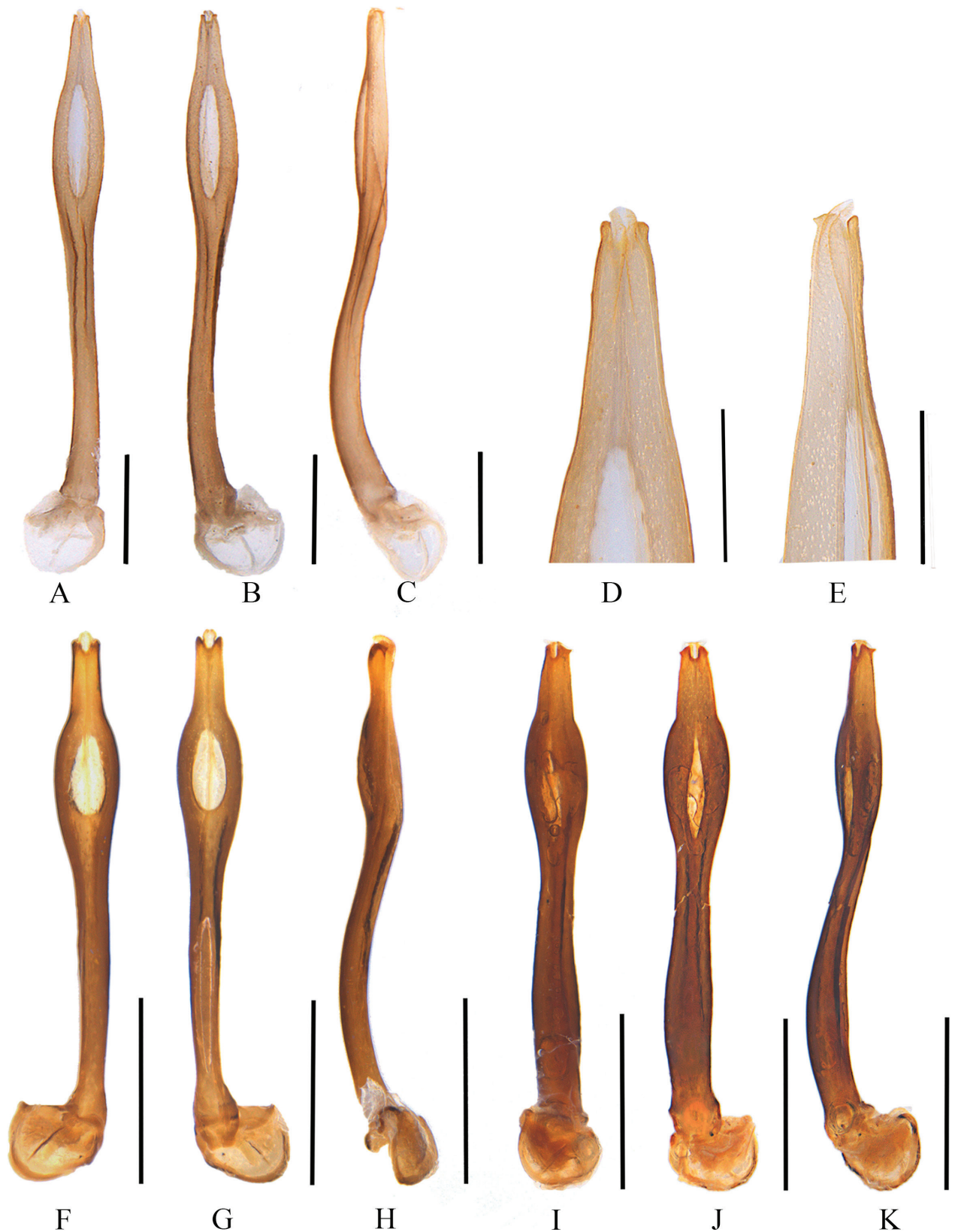
Figure 7. Aedeagi of *Macrolycus* species: **A–E** *M. aemulus* Barovskij, 1930; **F–H** *M. unicolor* **sp. nov.**; **I–K** *M. huoditangensis* **sp. nov.** A, D, F, I: dorsal views; B, G, J: ventral views; C, E, H, K: lateral views. Scale bars: A–C, F–K: 1.0 mm; D, E: 0.5 mm.

of ca. 130° between basal and apical parts of dorsal side, moderately arcuate at base part, subapical part strongly inflated dorsally (Figs 7K, 8A); moderately swollen at basal part in ventral view, subapical part strongly inflated laterally and almost symmetrical (Figs 7I, J, 8B), with a fusiform ventral cavity (Fig. 7J); apical part gradually narrowed distad (Fig. 7I, J), with a deep V-shaped notch at apex (Fig. 7J).

Female. Unknown.

Diagnosis. This species is more similar to *M. atronotatimimus* **sp. nov.** (described below) in the general shape of the median lobe but differs from the latter in the unicolored pronotum and in the stout median lobe, which is swollen at the basal part in ventral view (Figs 7J, 8B). In contrast, in *M. atronotatimimus* **sp. nov.**, the pronotum has a black patch in center of disc and median lobe are slender and parallel-sided at the basal part in ventral view (Figs 4J, K, 8B).

Etymology. The specific name is derived from its type locality, Huoditang, Shaanxi Province, China.

Distribution. China (Shaanxi).

Macrolycus atronotatimimus Y. Yang, Liu & X. Yang, sp. nov.

https://zoobank.org/E194DD1D-5CB6-429F-9DC9-FBEBD2321D56

Figures 4J–L, 5G, 6A, 8A, B

Type material. Holotype: China • ♂ (IZAS); Anhui, Jinzhai, Tiantangzhai, Tiantangzhai Scenic Spot; 952.56 m; 8.V.2021, K. D. Zhao & X. C. Zhu. leg.

Description. Male (Fig. 6A). Length 11.2 mm, width at humeri 2.3 mm. — Body black. Pronotum dark red with black median patch, elytra dark red. Surface covered with decumbent red pubescence. — Head relatively small. Eyes small, interocular distance approximately twice as large as eye diameter. Antennae (Fig. 5G) flabellate, overlapping two-thirds the length of the elytra when inclined. Antennomere II transverse; III–XI lamellate, pointed at apices, antennomere III with lamella nearly as long as joint itself; lamella of IX longest, 3.3 times longer than joint itself. — Pronotum trapezoidal, 1.25 times wider than long, disc present with a median longitudinal keel extending from anterior margin to middle part. Anterior margin weakly convex, lateral margins sinuate and posterior margin bisinuate; anterior angles rounded, posterior angles posterior angles sharp and prominently projected. Scutellum trapezoidal, feebly emarginate at apex. — Elytra slender and subparallel, 3.9 times longer than humeral width. Each elytron with four costae, costa I weak but visible in whole length; costae II and IV stronger than costa III; costa III visible only at basal part. — **Aedeagus:** median lobe slender, strongly curved near middle in lateral view, at an angle of ca. 120° between basal and apical parts of dorsal side, moderately arcuate at base part, subapical part moderately inflated dorsally (Figs 4L, 8A); parallel-sided at basal part in ventral view, subapical part strongly inflated laterally and almost symmetrical (Figs 4J, K, 8B), with a fusiform ventral cavity (Fig. 4J); apical part feebly swollen (Fig. 4J, K), with a deep U-shaped notch at apex (Fig. 4K).

Female. Unknown.

Diagnosis. This species resembles *M. atronotatus* in the shapes of pronotum and elytra but can be distinguished by the dark red pronotum and elytra (Fig. 6A), with orange pronotum and elytra in the latter. It also looks like *M. huoditangensis* **sp. nov.** but differs from the latter in the bicolored pronotum and slender median lobe, which is parallel-sided at the basal part in ventral view (Figs 4K, 8B). In comparison, the pronotum of *M. huoditangensis* **sp. nov.** is unicolored, and the median lobe is stout and swollen at the basal part in ventral view (Figs 7J, 8B).

Etymology. The specific name is derived from the Latin "*mimus*" (imitator), referring to its similarity to *M. atronotatus*.

Distribution. China (Anhui).

3.2. GM analyses of male genitalia shapes

Analyses of the datasets using TpsSmall indicated that excellent correlations between the tangent and the shape space in ventral and lateral views existed. The correlation (uncentered) between the tangent space (Y) regressed onto Procrustes distance (geodesic distances in radians) was 1.000000. There was little doubt on the basis of the result from TpsSmall, which supported the hypothesis that species within the *M. dotatus* species group can be analyzed by geometric morphometric methods because the results from the statistical test performed by TpsSmall proved the acceptability of the data for further statistical analysis (Pretorius and Scholtz 2001).

The first two principal components of the shape of the median lobe in lateral and ventral views explain 83.31% and 91.46% of the micromesh variation, respectively (Tables S1, S2). They were plotted to indicate variation along the first two relative warp axes, which were shown as deformations of the least squares reference using thin-plate splines in lateral (Fig. 8A) and ventral (Fig. 8B) views.

Comparison of the tps configurations indicated that the average shape of the median lobe of the *M. dotatus* species group is almost even in width except for being slightly narrowed at apical one-seventh, bisinuate at basal nine- and three-fourteenths, respectively, and accordingly at an angle of ca. 30° and 150° with apical part in lateral view (Fig. 8a); nearly straight along whole length, subparallel-sided at basal four-sevenths, roundly and asymmetrically widened laterally at apical two-sevenths, gradually narrowed at apical one-seventh, feebly and triangularly emarginated at apex in ventral view (Fig. 8b).

The PCA and CVA scatter plots of shape differences of the shape of median lobe in lateral and ventral views (Figs S1–S4) showed that each species of *M. dotatus* species-group independently occupied an area and separated from one another.
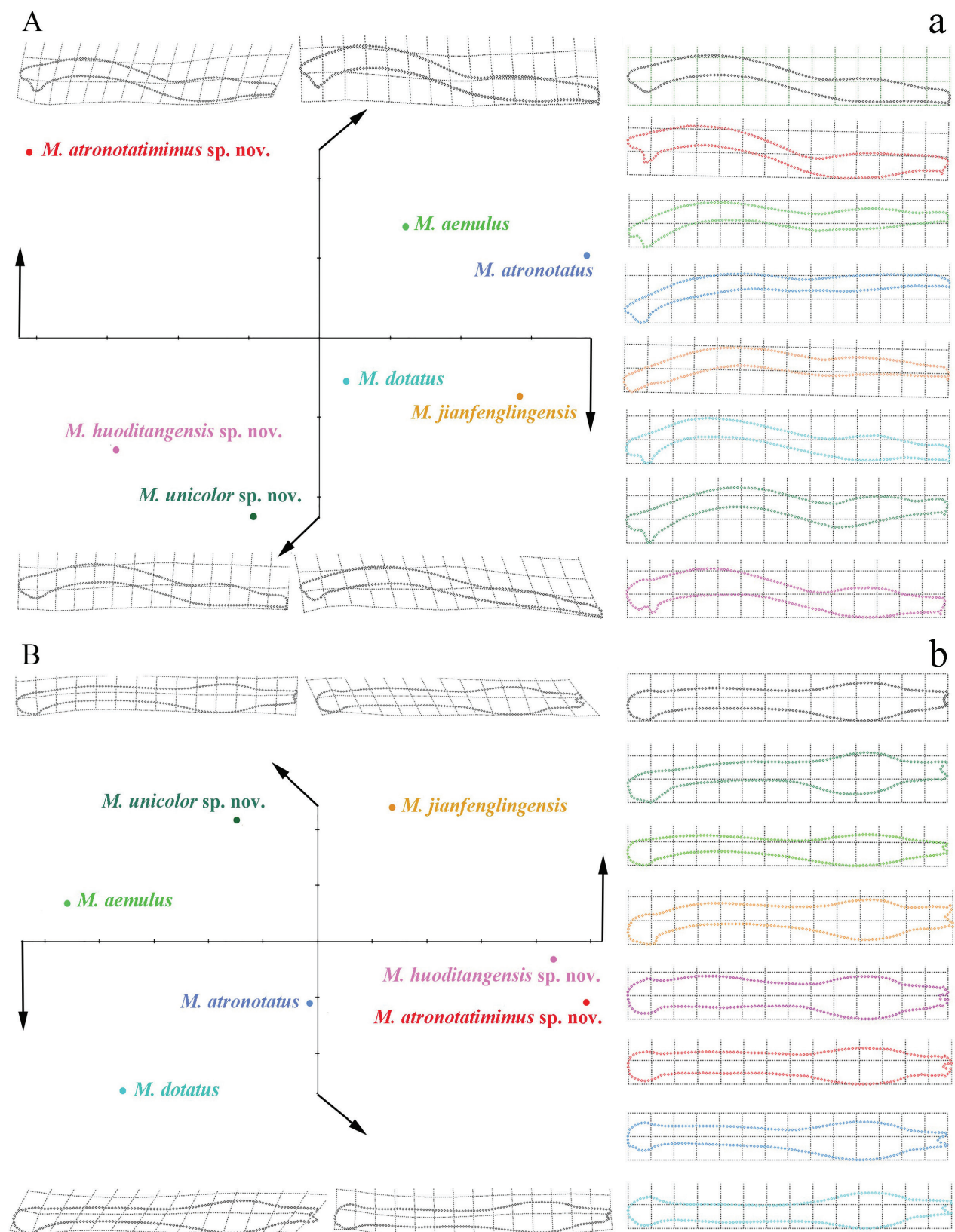
Figure 8. Differences in the shape of the median lobe of the *Macrolycus dotatus* species group in relative warps computed from the dataset in lateral (**A**) and ventral (**B**) views, plotted against one another to indicate positions of the relationships among the species. The shape changes of different species implied by variation along the first two relative warp axes. Shape changes are shown as deformation of the GLS reference, using tps configurations. The reference configurations (situated at the origin) shown in lateral (**a**) and dorsal (**b**) views, those at the left, right, top and bottom are indicated by arrows, and each species is represented by a different color.
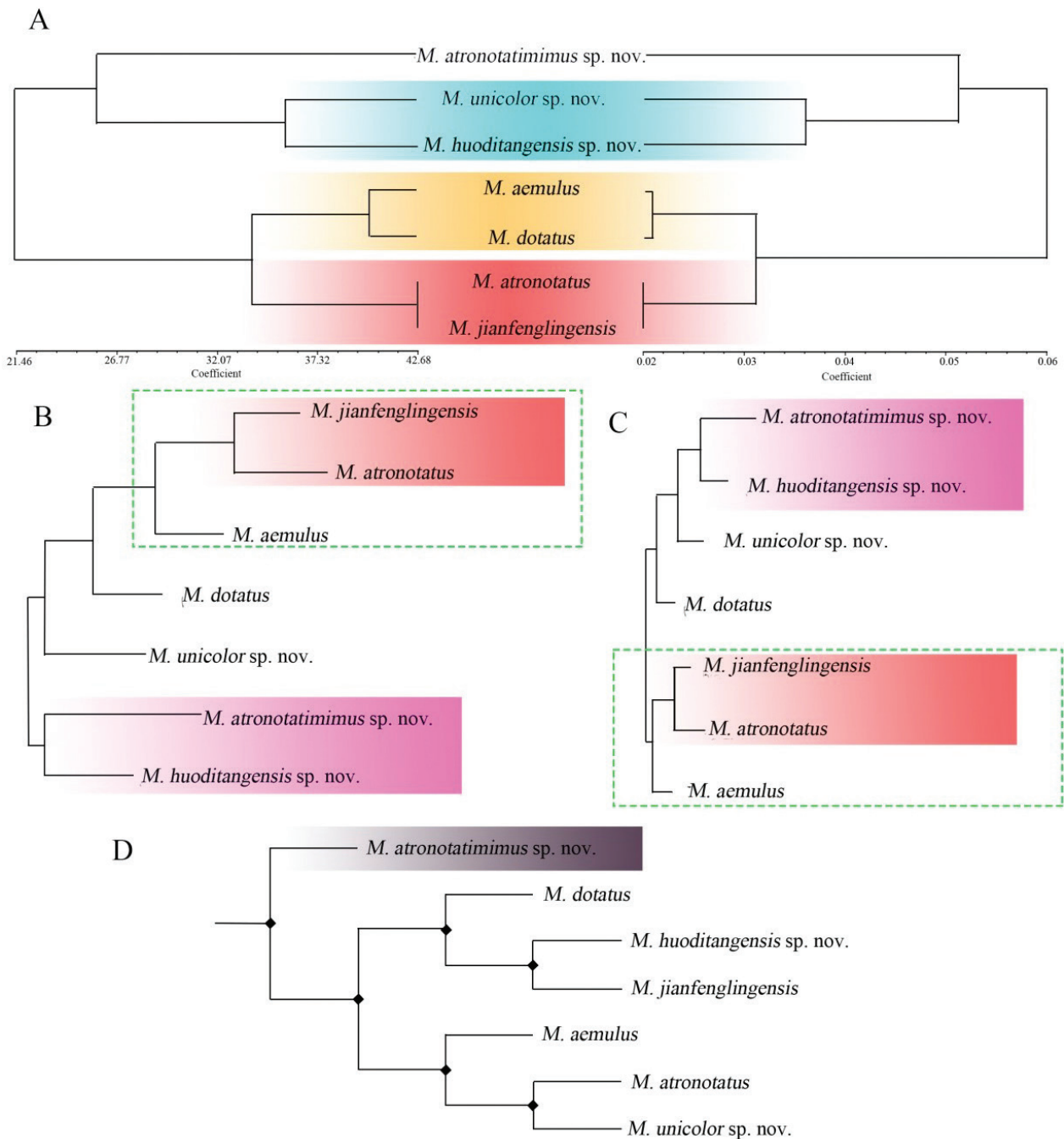
Figure 9. Topologies of the *Macrolycus dotatus* species group based on the shape of the median lobe in lateral view: **A** Phenograms based on the Mahalanobis distances (left) and Procrustes distances (right) using UPGMA; **B–C** NJ trees based on Mahalanobis distances (B) and Procrustes distances (C) with 1000 bootstrap replicates; D. Phylogenetic hypothesis based on two landmark configurations using MP analysis. The branches in different colors or dashed boxes represent the same clade recovered in different phenograms.

3.3. PM analyses based on male genitalia shapes

The UPGMA phonograms based on both Procrustes and Mahalanobis distances of the shape of the median lobe in lateral view were completely consistent with each other (Fig. 9A). The species of the *M. dotatus* species group were divided into two branches, one of which was composed of *M. atronotatimimus* **sp. nov.** + (*M. unicolor* **sp. nov.** + *M. huoditangensis* **sp. nov.**), and the other consisted of (*M. aemulus* + *M. dotatus*) + (*M. atronotatus* + *M.*

jianfenglingensis). In both NJ trees (Fig. 9B, C), the clade of *M. atronotatus* + *M. jianfenglingensis* was recovered, but it was clustered only with *M. aemulus*. In contrast to the UPGMA results, *M. atronotatimimus* **sp. nov.** and *M. huoditangensis* **sp. nov.** were always grouped into a clade in the NJ trees.

However, the produced topology of the MP analysis (Fig. 9D) is totally different from the aforementioned relationships among the species. The shape of the median lobe of *M. atronotatimimus* **sp. nov.** is the most distinctive, which can also be reflected by its position in the rel-
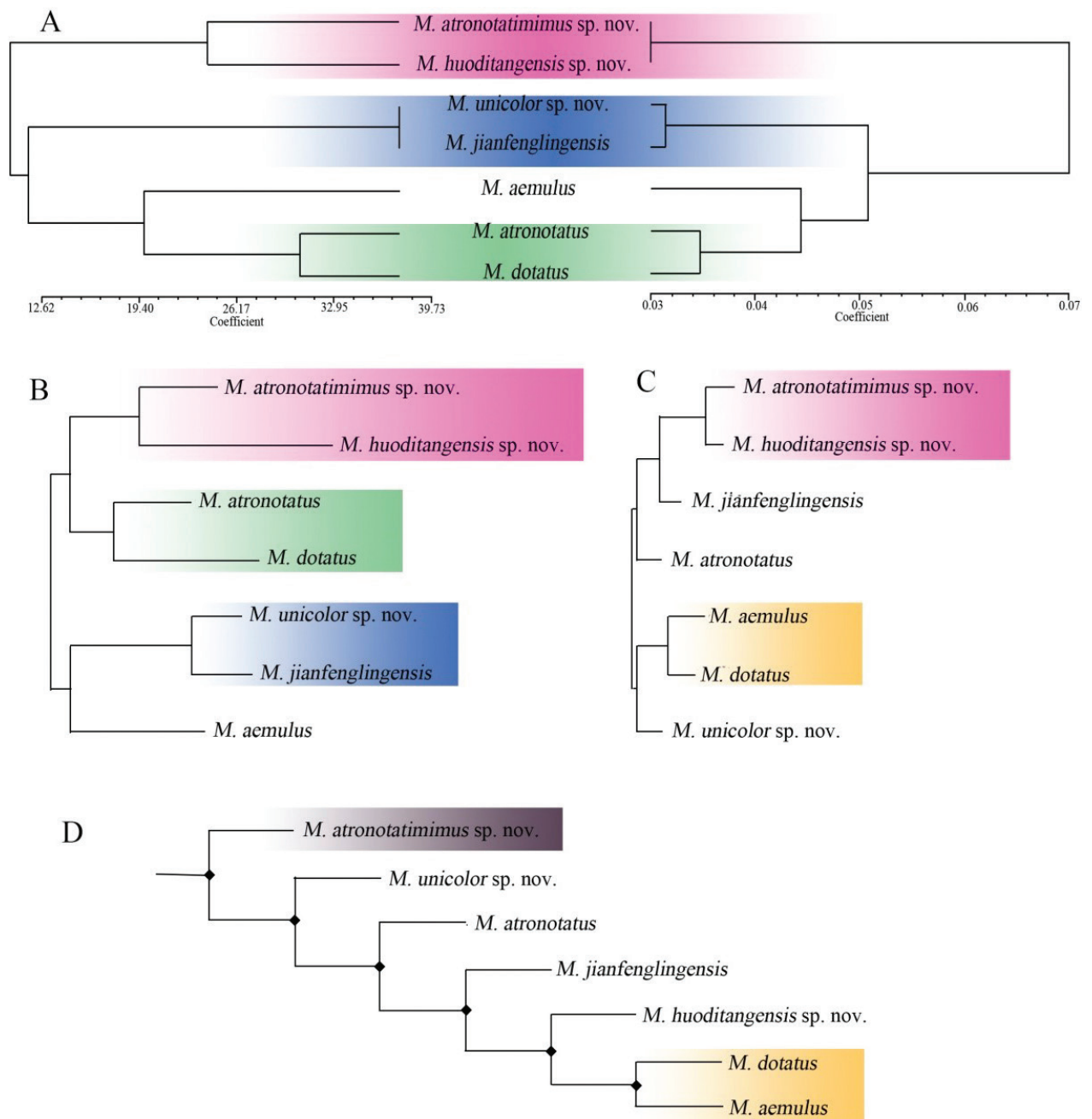
Figure 10. Topologies of the *Macrolycus dotatus* species group based on the shape of the median lobe in ventral view: **A** Phenograms based on the Mahalanobis distances (left) and Procrustes distances (right) using UPGMA; **B–C** NJ trees based on Mahalanobis distances (B) and Procrustes distances (C) with 1000 bootstrap replicates; D. Phylogenetic hypothesis based on two landmark configurations using MP analysis. The branches in different colors represent the same clade recovered in different phenograms.

ative warp axis. It occupies the top left position of the relative warp axis in the lateral view of the median lobe (Fig. 8A: tps configuration in red coloration). If *M. atronotatimimus* **sp. nov.** was at the basal clade, the remaining species were grouped into two clusters, of which one was recovered as *M. dotatus* + (*M. huoditangensis* **sp. nov.** + *M. jianfenglingensis*) and the other as *M. aemulus* + (*M. atronotatus* + *M. unicolor* **sp. nov.**).

Similar to the above, the clade of *M. atronotatimimus* **sp. nov.** + *M. huoditangensis* **sp. nov.** was recovered in both UPGMA phonograms (Fig. 10A) and NJ trees (Fig. 10B, C) based on the morphometric data of the shape of

the median lobe in ventral view. Additionally, *M. atronotatimimus* **sp. nov.** was the first to separate from all others in the phylogenetic tree of MP analysis (Fig. 10D) because it was located at the rightmost position in the ventral view (Fig. 8B: tps configuration in red coloration). In contrast, the clades of *M. unicolor* **sp. nov.** + *M. jianfenglingensis* and *M. atronotatus* + *M. dotatus* were clustered in both UPGMA phenograms (Fig. 10A) and the NJ tree of Mahalanobis distance (Fig. 10B). Meanwhile, the sister group of *M. aemulus* + *dotatus* was recovered in both the NJ tree of Procrustes distance (Fig. 10C) and the MP tree (Fig. 10D).

4. Discussion

4.1 Separate status of the new species

Similar to other net-winged beetles, the variability in the general appearance of *Macrolycus* sometimes prevents reliable identification (Li et al. 2012); therefore, the delineations of species are regularly based on the shape of the male genitalia and antennae, which are provided here in the following key. Although the shape of male genitalia is clearly defined in most cases, morphological interspecific divergence in quantitative variation is identified. Geometric morphometrics is a rigorous method (Gilchrist et al. 2000; Debat et al. 2003) to find and analyze shape variations between species (Walker 2000), thereby facilitating and stabilizing the taxonomy of *Macrolycus*. In addition, coloration patterns are rarely conspicuously variable within species (Li et al. 2012) due to their signaling function for unpalatability (Bocak and Bocakova 2008), so they will also be applied in the key.

Key to the species of the *Macrolycus dotatus* species group

1 Median lobe of aedeagus strongly curved near the middle in lateral view, at an angle of less than 130° between basal and apical parts of dorsal side (Figs 4L, 7H, 7K, 8A) **2**

1' Median lobe of aedeagus moderately or feebly curved near the middle in lateral view, at an angle of more than 150° between basal and apical parts of dorsal side (Figs 4C, 4F, 4I, 7C, 8A)..**4**

2 Pronotum and elytra uniformly orange (Fig. 6B); median lobe of aedeagus feebly curved at basal part, at an angle of ca. 15° with apical part in ventral view, subapical part asymmetrically inflated (Figs 7G, 8B) ....
....***M. unicolor* Y. Yang, Liu & X. Yang, sp. nov.**

2' Pronotum and elytra dark red and/or with a black patch in center of pronotal disc; median lobe of aedeagus nearly straight at basal part, in a horizontal line with apical part in ventral view, subapical part almost symmetrically inflated (Figs 4K, 7J, 8B)..**3**

3 Pronotum unicolored; median lobe of aedeagus stout, swollen at basal part in ventral view (Figs 7J, 8B).............
.... ***M. huoditangensis* Y. Yang, Liu & X. Yang, sp. nov.**

3' Pronotum with a black patch in center of disc (Fig. 6A); median lobe of aedeagus slender, parallel-sided at basal part in ventral view (Figs 4K, 8B) ....***M. atronotatimimus* Y. Yang, Liu & X. Yang, sp. nov.**

4 Median lobe of aedeagus moderately curved near middle in lateral view, at an angle of ca. 150° between basal and apical parts of dorsal side (Figs 4I, 7C, 8A) **5**

4' Median lobe of aedeagus feebly curved near middle in lateral view, nearly in a horizontal line between basal and apical parts of dorsal side (Figs 4C, 4F,, 8A)...**6**

5 Pronotum and scutellum black; pronotum distinctly wider than long, with posterior angles obviously projecting postero-laterally, acute at apices (Fig. 3D); median lobe of aedeagus moderately curved at basal part in ventral view, subapical part moderately inflated (Figs 7B, 8B).. ***M. aemulus* Barovskij, 1930**

5' Pronotum and scutellum orange; pronotum nearly as wide as long, with posterior angles feebly projecting postero-laterally, subrectangular at apices (Fig. 3C); median lobe of aedeagus nearly straight at basal part in ventral view, subapical part strongly inflated (Figs 4H, 8B)...***M. dotatus* Kleine, 1925**

6 Pronotum, scutellum and elytra uniformly dark red (Fig. 3B); male antennomere III with lamella 0.8 times as long as joint itself (Fig. 5B); median lobe of aedeagus obviously curved at base in ventral view (Figs 4E, 8B) ....
....***M. jianfenglingensis* Li, Bocak & Pang, 2015**

6' Pronotum orange, with a black patch in center of disc, scutellum black, elytra orange (Fig. 3A); male antennomere III with lamella 1.2 times longer than joint itself (Fig. 5A); median lobe of aedeagus almost parallel-sided at basal part in ventral view (Figs 4B, 8B) ....***M. atronotatus* Pic, 1939**

4.2 Male genitalia shapes in delineation of species

In the present study, the statistical test performed by TpsSmall suggested that our obtained data of male genitalia are acceptable for the geometric morphometric analysis. Furthermore, the CVA analysis suggested that all species of the *M. dotatus* species group can be distinguished from one another by the shape of male genitalia, which is consistent with the preceding part in the key combined with some nongenital characteristics.

Male genitalia are undoubtedly among the most important and versatile morphological characteristics in insect taxonomy (Tuxen 1970; Song and Bucheli 2010). Male genitalia possess many traits that are unique to species, especially among closely related species, and their utility in species diagnosis has been thoroughly proven in many groups (Eberhard 1985; Hosken and Stockley 2004). A general consensus in the study of genital evolution is that male genitalia are under sexual selection (Eberhard 1985, 2001, 2004b; Huber and Eberhard 1997; Arnqvist 1998; Arnqvist and Danielsson 1999; Córdoba-Aguilar 2005; House and Simmons 2005). Because sexually selected characters tend to evolve rapidly (Lande 1981; Kirkpatrick 1982; West-Eberhard 1983; Gavrilets 2000), researchers generally agree that male

genitalia evolve both rapidly and divergently (Eberhard 1985; Arnqvist 1997; Hosken and Stockley 2004; Mendez and Cordoba-Aguilar 2004). It is also a logical conclusion from the observation that male genitalia are consistently useful as a taxonomic character at the specific level, which suggests that they acquire a new form in each new species (Eberhard 1985). This assumption was verified in our study, and the species of the *M. dotatus* species group can be successfully delineated by the shape of male genitalia. In other words, the three new species discovered here have different median lobe shapes from the previously known species. Although only quantitative variations are exhibited, their differences are shown clearly in the tps configurations by GM methods. Moreover, the species that have no or only simple descriptions of male genitalia in previous publications (Pic 1923, 1935; Kleine 1925, 1933, 1942; Nakane 1967, 1969; Kazantsev 1993, 2001, 2002, 2011; Li et al. 2012, 2015) could be described in more detail. Therefore, we provide detailed descriptions of male genitalia for the *M. dotatus* species group in taxonomy Part 3.1, and combined with the results of Part 4.3, we could make comparisons between the new species and other similar species in this structure.

4.3   Phenetic relationships based on male genitalia shapes in different views

The clades of *M. atronotatimimus* **sp. nov.** + *M. huoditangensis* **sp. nov.** and *M. aemulus* + *M. dotatus* are frequently recovered based on the shape of the median lobe in both lateral (Figs 9B, C and 10A–C) and ventral (Figs 9A, 10C, D) views by either UPGMA or NJ analyses. These results suggest that the paired species have the most similar male genitalia. It is no doubt that this could be integrated in the description of taxonomy part.

Except for the common clades, there are some clades recovered solely in either lateral or ventral view. *M. atronotatus* + *M. jianfenglingensis* (Fig. 9A–C), which together are closer to *M. aemulus* (Fig. 9A, B), and *M. unicolor* **sp. nov.** + *M. huoditangensis* **sp. nov.** (Fig. 9A) are recovered only in lateral view. In comparison, *M. unicolor* **sp. nov.** + *M. jianfenglingensis* (Fig. 10A, B) and *M. atronotatus* + *M. dotatus* (Fig. 10A, B) are solely produced in ventral view. These inconsistencies resulted from the independent analysis of the shape of the median lobe in different views. In the present study, only 2-dimensional visualization of the shape of the median lobe was analyzed. Although it provides a well-defined outline, the median lobe is actually a 3-dimensional structure, which demands data analysis to be conducted integrally. Therefore, more techniques are required to obtain and thoroughly analyze the 3-dimensional shape of the median lobe in the future, such as microcomputed tomography (or μ-CT) and computer-based 3D reconstruction techniques. Then, we can apply these comprehensive data in a phylogenetic context by combining GM and MP methods.

4.4.   Topologies produced by morphometric and molecular data

In the molecular phylogeny of Li et al. (2015), four species of the *M. dotatus* species group were included in the analysis, and the phylogenetic relationships were recovered as (*M. jianfenglingensis* + *M. dotatus*) + (*M. atronotatus* + *Macrolycus* sp.). In the present study, we analyzed a total of seven species on the basis of the shape of the median lobe by combining the GM and MP methods. The phylogenetic relationships inferred from MP analyses (Figs 9D, 10D) are consistent with the above molecular phylogeny, with a closer relationship between *M. jianfenglingensis* and *M. dotatus* than *M. atronotatus*, but the converse (Figs 9A–C, 10C) or the latter two closer (Fig. 10A, B) in UPGMA and NJ analyses. The discrepancy in the topologies probably results from different analysis data and optimality criteria of the methods.

Currently, molecular phylogenetics has become the standard for inferring evolutionary relationships (Ziemert and Jensen 2012). Because numerous genes with fundamental biochemical functions are present in all species, they can be sequenced, aligned, and analyzed to study phylogenetic relationships at the deepest part of the tree of life (Hillis and Dixon 1991). In addition, this relationship appeared to be robust to tree-building methods. Therefore, the phylogenetic relationship inferred from the molecular data can be used as the standard reference (Zhao et al. 2023), and the study of Li et al. (2015) is no exception.

In morphological phylogenies, male genitalia have been broadly used across diverse arthropod lineages by systematists (Song and Bucheli 2010). Male genitalia provide excellent phylogenetic signals in higher-level classifications of several insect orders (Sharp and Muir 1912; Eyer 1924; Peck 1937; Michener 1944; Zumpt and Heinz 1950; Snodgrass 1957; Roth 1970). However, at the specific level, there is an idea that the rate of genital evolution is extremely rapid, to the point that there may not be observable phylogenetic inertia left in the structures (Arnqvist and Rowe 2002; Eberhard 2004a). In contrast, Song and Bucheli (2010) argued that rapid evolution does not necessarily equate to the lack of phylogenetic signal, and characters that evolve by a pattern of descent with modification make appropriate characters for a phylogenetic analysis, regardless of the rate of evolution, so they stated that male genitalia have phylogenetically conserved components at a deeper level (between families) as well as at a shallow level (between species).

Unexpectedly, there is still a gap between our obtained results of UPGMA and NJ analyses (Figs 9A–C, 10A–C) and the previous molecular phylogeny (Li et al., 2015). The most important advantage of using Procrustes and/or Mahalanobis distances to capture shape variation was that these distances were considered the best method for measuring shape differences among taxa (Goodall and Bose 1987; Chapman 1990; Rohlf 1990; Goodall 1991; Marcus et al. 1993; Pretorius and Scholtz 2001). Thus, the Procrustes and/or Mahalanobis distances can effectively indicate phenetic relationships, summarizing over-

all patterns of similarity (Pretorius and Scholtz 2001; Zhao et al. 2023). However, Losos (1999) argued that no relationship may exist between the degree of phylogenetic relationship and phenotypic similarity if rates of character evolution are high relative to the speciation rate. In this case, it is supposed that some nongenital characters of male (Song and Bucheli 2010) or female genitalia (Simmons and Fitzpatrik 2019) are also involved in the speciation of *Macrolycus*. Although the phenotypic similarity is different from those deepest in the molecular tree, it provides useful information for us to recognize morphologically similar species. Meanwhile, the tps configurations of GM analysis allow us to make quantitative comparisons among the species in terms of morphology.

Nevertheless, the phylogenetic relationships based on the geometric morphometric data of the shape of the median lobe by MP analysis are comparable to the molecular phylogenetic results, so it is possible to explore the relationships when DNA data are unavailable.

5. Conclusion

In the present study, we review the lycid *Macrolycus dotatus* species group and describe three new species from China, including *M. unicolor* **sp. nov.**, *M. huoditangensis* **sp. nov.** and *M. atronotatimimus* **sp. nov.** Then, we analyze the shape of the median lobe of this group using the GM method and further investigate the phenotypic relationships among the species based on these morphometric data by UPGMA, NJ and MP analyses. The results of PCA and CVA analyses suggest that all species of the *M. dotatus* species group could be well delineated by male genitalia. The produced phenograms frequently recover phenotypic similarity between the coupled species, including *M. atronotatimimus* **sp. nov.** + *M. huoditangensis* **sp. nov.** and *M. aemulus* + *M. dotatus*, which are similar in the shape of the median lobe in both ventral and lateral views. In addition, some species were similar in either the ventral or lateral view. These results are helpful for making comparisons among the species in the shape of the median lobe exhibiting only quantitative variation, which is particularly useful for the description of new species. Meanwhile, the MP analysis of male genitalia shape using two landmark configurations is considered reliable in inferring the phylogenetic relationship among species because of the consistency between its topologies and the molecular phylogeny, with a closer relationship between *M. jianfenglingensis* and *M. dotatus* than *M. atronotatus*. *M. atronotatimimus* **sp. nov.** is considered the most distinctive species by its characteristic shape of the median lobe, which is distinctly different from all others. Nevertheless, more data (molecular or 3D-morphometric) are required in the future to reassess the phylogenetic relationships of the *M. dotatus* species group and to verify the obtained results of the present study.

This study will shed new light on the morphological taxonomy of insects on lower grades while fully utilizing the taxonomic value of the male genitalia; in particular, it will provide some inspiration to obtain a more dependable phylogeny among those taxa if they are unavailable with molecular data.

8. References

Adams DC, Rohlf FJ, Slice DE (2004) Geometric morphometrics: Ten years of progress following the 'revolution'. Italian Journal of Zoology 71(1): 5–16. https://doi.org/10.1080/11250000409356545

Arnqvist G (1997) The evolution of animal genitalia: distinguishing between hypotheses by single species studies. Biological Journal of the Linnean Society 60(3): 365– 379. https://doi.org/10.1111/j.1095-8312.1997.tb01501.x

Arnqvist G (1998) Comparative evidence for the evolution of genitalia by sexual selection. Nature 393: 784–786.

Arnqvist G, Danielsson I (1999) Copulatory behavior, genital morphology, and male fertilization success in water striders. Evolution 53: 147–156.

Arnqvist G, Rowe L (2002) Correlated evolution of male and female morphologies in water striders. Evolution 56: 936–947.

Aytekin MA, Terzo M, Rasmont P, Çağatay N (2007) Landmark based geometric morphometric analysis of wing shape in *Sibiricobombus* Vogt (Hymenoptera: Apidae: *Bombus* Latreille). Annales de la Société entomologique de France 43(1): 95–102. https://www.webofscience.com/wos/alldb/full-record/WOS:00024534580 0012

Barovskij VV (1930) Description d'une nouvelle espèce du genre *Macrolycus* Waterh. (Coleoptera, Lycidae). Comptes Rendus de l'Académie des Sciences de l'URSS 1: 580–581.

Baylac M, Villemant C, Simbolotti G (2003) Combining geometric morphometrics with pattern recognition for the investigation of species complexes. Biological Journal of the Linnean Society 80(1): 89–98. https://doi.org/10.1046/j.1095-8312.2003.00221.x

Bocak L, Bocakova M (1990) Revision of the supergeneric classification of the family Lycidae (Coleoptera). Polskie Pismo Entomologiczne 59(4): 623–676.

Bocak L, Bocakova M (2008) Phylogeny and classification of the family Lycidae (Insecta: Coleoptera). Annales Zoologici 58(4): 695–720. https://doi.org/10.3161/000345408X396639

Bookstein FL (1991) Thin-Plate splines and the atlas problem for biomedical images. In: Colchester ACF, Hawkes DJ (eds) Informa-

tion Processing in Medical Imaging. IPMI 1991. Lecture Notes in Computer Science, Springer, Berlin, Heidelberg, 511pp. https://doi.org/10.1007/BFb0033763

Brancucci M (1980) Morphologie comparée, évolution et systématique des Cantharidae (Insecta: Coleoptera). Entomologica Basiliensia 5: 215–388.

Champakaew D, Junkum A, Sontigun N, Sanit S, Limsopatham K, Saeung A, Somboon P, Pitasawat B (2021) Geometric morphometric wing analysis as a tool to discriminate female mosquitoes from different suburban areas of Chiang Mai province, Thailand. PloS one 16(11): e0260333. https://doi.org/10.1371/journal.pone.0260333

Chapman RE (1990) Conventional Procrustes approaches. In: Rohlf FJ, Bookstein FL (Eds) Proceedings of the Michigan Morphometrics Workshop. University of Michigan, Museum of Zoology Special Publication Ann Arbor 2: 251–267.

Córdoba-Aguilar A (2005) Possible coevolution of male and female genital form and function in a calopterygid damselfly. Journal of Evolutionaty Bology 18: 132–137. https://doi.org/10.1111/j.1420-9101.2004.00796.x

Debat V, Bégin M, Legout H, David JR (2003) Allometric and nonallometric components of *Drosophila* wing shape respond differently to developmental temperature. Evolution 57: 2773–2784. https://doi.org/10.1111/j.0014-3820.2003.tb01519.x

De la Riva J, Le Pont F, Al V, Matias A, Mollinedo S, Dujardin JP (2001) Wing geometry as a tool for studying the *Lutzomyia longipalpis* (Diptera: Psychodidae) complex. Memórias do Instituto Oswaldo Cruz 96(8): 1089–1094. https://doi.org/10.1590/S0074-02762001000800011

Díaz-Cruz JA, Alvarado-Ortega J, Ramírez-Sánchez MM, Bernard EL, Allington-Jones L, Graham M (2021) Phylogenetic morphometrics, geometric morphometrics and the Mexican fossils to understand evolutionary trends of enchodontid fishes. Journal of South American Earth Sciences 111: 103492. https://doi.org/10.1016/j.jsames.2021.103492

Dujardin JP, Le Pont F, Baylac M (2003) Geographical versus interspecific differentiation of sand flies (Diptera: Psychodidae): a landmark data analysis. Bulletin of entomological research 93(1): 87–90. https://doi.org/10.1079/BER2002206

Eberhard WG (1985) Sexual Selection and Animal Genitalia. Cambridge: Harvard University Press.

Eberhard WG (2001) Species-specific genitalic copulatory courtship in sepsid flies (Diptera, Sepsidae, *Microsepsis*) and theories of genitalic evolution. Evolution 55: 93–102.

Eberhard WG (2004a) Male–female conflict and genitalia: failure to confirm predictions in insects and spiders. Biological Reviews 79: 121–186. https://doi.org/10.1017/S1464793103006237

Eberhard WG (2004b) Rapid divergent evolution of sexual morphology: comparative tests of antagonistic coevolution and traditional female choice. Evolution 58: 1947–1970.

Eyer JR (1924) The comparative morphology of the male genitalia of the primitive Lepidoptera. Annals of The Entomological Society of America 17: 275– 328. https://doi.org/10.1093/AESA/17.3.275

Faille A, Déliot P, Quéinnec E (2007) A new cryptic species of *Aphaenops* (Coleoptera: Carabidae: Trechinae) from a French Pyrenean cave: congruence between morphometrical and geographical data confirm species isolation. Annales de la Société Entomologique de France (n.s.) 43(3): 363–370. https://doi.org/10.1080/00379271.2007.10697533

Francuski L, Ludoški J, Vujić A, Milankov V (2009) Wing geometric morphometric inferences on species delimitation and intraspecific

divergent units in the *Merodon ruficornis* group (Diptera, Syrphidae) from the Balkan Peninsula. Zoological Science 26(4): 301–308. https://doi.org/10.2108/zsj.26.301

Gavrilets S (2000) Rapid evolution of reproductive barriers driven by sexual conflict. Nature 403: 886–889.

Gilchrist AS, Azevedo RBR, Partridge L, Higgins PO' (2000) Adaptation and constraint in the evolution of *Drosophila melanogaster* wing shape. Evolution & Development 2(2): 114–124. https://doi.org/10.1046/j.1525-142x.2000.00041.x

Goloboff P, Catalano S (2016) TNT v.1.5, including a full implementation of phylogenetic morphometrics. Cladistics 32: 221–238. https://doi.org/10.1111/cla.12160

Goodall CR (1991) Procrustes methods in the statistical analysis of shape. Journal of the Royal Statistical Society 53: 285–339. https://doi.org/10.1111/j.2517-6161.1991.tb01825.x

Goodall CR, Bose A (1987) Procrustes techniques for the analysis of shape and shape change. In: Heiberger R (Ed.) Computer Science and Statistics: Proceedings of the 19th Symposium on the Interface. American Statistical Association, Alexandria, Virginia, 86–92.

Hájek J, Fikáček M (2010) Taxonomic revision of the *Hydroporus bodemeyeri* species complex (Coleoptera: Dytiscidae) with a geometric morphometric analysis of body shape within the group. Journal of Natural History 44(27–28): 1631–1657. https://doi.org/10.1080/00222931003760053

Hillis DM, Dixon MT (1991) Ribosomal DNA: Molecular Evolution and Phylogenetic Inference. The Quarterly Review of Biology 66(4): 411–453. https://www.journals.uchicago.edu/doi/abs/10.1086/417338

Hosken DJ, Stockley P (2004) Sexual selection and genital evolution. Trends in Ecology & Evolution 19(2):87–93. https://doi.org/10.1016/j.tree.2003.11.012

House CM, Simmons LW (2005) The evolution of male genitalia: patterns of genetic variation and covariation in the genital sclerites of the dung beetle *Onthophagous* taurus. Journal of Evolutionaty Biology 18: 1281–1292. https://doi.org/10.1111/j.1420-9101.2005.00926.x

Huber BA, Eberhard WG (1997) Courtship, copulation, and genital mechanics in *Physocyclus globosus* (Araneae, Pholcidae). Canadian Journal of Zoology 75(6): 905–918. https://doi.org/10.1139/z97-109

Kazantsev SV (1993b) Lycides nouveaux ou peu connus de l'Indochine (Coleoptera). Bulletin du Muséum National d'Histoire naturelle (Paris) A 15(4): 49–68.

Kazantsev SV (2001) *Macrolycus* Waterhouse, 1878 (Coleoptera: Lycidae) of continental China. Elytron 14 (2000): 99–109.

Kazantsev SV (2002) New and little-known species of Lycidae (Coleoptera) from China. Russian Entomological Journal 11: 253–263.

Kazantsev SV (2011) An annotated checklist of Cantharoidea (Coleoptera) of Russia and adjacent territories. Russian Entomological Journal 20(4): 387–410. https://doi.org/10.15298/rusentj.20.4.05

Kirkpatrick M (1982) Sexual selection and the evolution of female choice. Evolution 36: 1–12.

Kleine R (1925) Die Gattung *Macrolycus* C. O. Wtrh. (5. Beitrag zur Kenntnis der Lycidae). Deutsche Entomologische Zeitschrift 4: 325–331.

Kleine R (1933) Neue Lyciden und Bemerkungen zum Cat. Col. Junk-Schenkling Lycidae. Stettiner Entomologische Zeitung 94: 1–20.

Kleine R (1942) Bestimmungstabelle der Lycidae. In Bestimmungstabellen der europäischen Coleopteren. 123. Heft. Troppau: Edmund Reitter, 90 pp.

Klingenberg CP (2010) Evolution and development of shape: integrating quantitative approaches. Nature Reviews. Genetics 11(9): 623–635. https://doi.org/10.1038/nrg2829

Klingenberg CP (2011) MorphoJ: an integrated software package for geometric morphometrics. Molecular Ecology Resources 11(2): 353–357. https://doi.org/10.1111/j.1755-0998.2010.02924.x

Kraatz G (1879) Neue Käfer vom Amur. Deutsche Entomologische Zeitschrift 23: 121–144.

Lande R (1981) Models of speciation by sexual selection on polygenic traits. Proceedings of the National Academy of Sciences of the United States of America 78(6): 3721–3725. https://doi.org/10.1073/pnas.78.6.3721

Li Y (2015) Molecular phylogeny and taxonomy of the tribes Macrolycini and Lyponiini (Coleoptera: Lycidae). Master thesis, Sun Yat-sen University, Guangzhou, China (unpublished).

Li Y, Pang H, Bocak L (2012) New species of *Macrolycus* Waterhouse, 1878 from China and Laos, with a checklist of the genus (Coleoptera: Lycidae). Zootaxa 3232: 44–61. https://doi.org/10.11646/zootaxa.3232.1.2

Li Y, Pang H, Bocak L (2015) Molecular phylogeny of *Macrolycus* (Coleoptera: Lycidae) with description of new species from China. Entomological Science 18: 319–329. https://doi.org/10.1111/ens.12133

Li L, Qi Y, Yang Y, Bai M (2016) A new species of *Falsopodabrus* Pic characterized with geometric morphometrics (Coleoptera, Cantharidae). ZooKeys 614: 97–112. https://doi.org/10.3897/zookeys.614.6156

Losos JB (1999) Uncertainty in the reconstruction of ancestral character states and limitations on the use of phylogenetic comparative methods. Animal Behavior 58: 1319–1324.

Marcus LF, Bello E, García-Valdecasas A (1993) Contributions to morphometrics (Vol. 8). Contributions to Morphometrics. Museo Nacional de Ciencias Naturales, Consejo Superior de Investigaciones Científicas, Madrid: 264.

Masek M, Motyka M, Kusy D, Bocek M, Li Y, Bocak L (2018) Molecular Phylogeny, Diversity and Zoogeography of Net-Winged Beetles (Coleoptera: Lycidae). Insects 9: 154. https://doi.org/10.3390/insects9040154

Matias A, De la Riva JX, Torrez M, Dujardin JP (2001) *Rhodnius robustus* in Bolivia identified by its wings. Memorias do Instituto Oswaldo Cruz 96(7): 947–950. https://doi.org/10.1590/S0074-02762001000700010

Mendez V, Cordoba-Aguilar A (2004) Sexual selection and animal genitalia. Trends in Ecology & Evolution 19: 224–225.

Michener CD (1944) A comparative study of the appendage of the eighth and ninth abdominal segments of insects. Annals of the Entomological Society of America 37: 336–351.

Nakane T (1967) Notes on the genus *Macrolycus* Waterhouse in Japan and Formosa (Coleoptera, Lycidae). Fragmenta Coleopterologica 17: 69–7.

Nakane T (1969) Lycidae (Insecta, Coleoptera). Fauna Japonica, Acadamic Press of Japan, Tokyo, 224 pp.

Peck O (1937) The male genitalia in the Hymenoptera, especially the family Ichneumonidae. I, II. Canadian journal of research: 11, 12. https://dx.doi.org/10.1139/cjr37d-019

Pretorius E, Scholtz CH (2001) Geometric morphometries and the analysis of higher taxa: a case study based on the metendosternite of the Scarabaeoidea (Coleoptera). Biological Journal of the Linnean Society 74: 35–50. https://doi.org/10.1111/j.1095-8312.2001.tb01375.x

Pic M (1923) Etude des Malacodermes de l'Indochine recueillis par M. R. Vitalis de Salvaza. Faune Entomologique de l'Indochine Française 1: 7–24.

Pic M (1935) Contribution à l'étude des coléoptères malacodermes. Annales de la Société Entomologique de France 104: 109–115.

Pic M (1939) Malacodermes exotiques. L'Échange, Revue Linnéenne 55(475–477): 165–172.

Roggero A, Passerin D'Entreves P (2005) Geometric morphometric analysis of wings variation between two populations of the *Scythris obscurella* species-group: geographic or interspecific differences? (Lepidoptera: Scythrididae). Shilap. Sociedad Hispano-Luso-Americana de Lepidopterología 33: 101–112.

Rohlf FJ (1990) The analysis of shape variation using ordinations of fitted functions. In: Sorensen JT, Foottit R (eds) Ordinations in the Study of Morphology, Evolution and systematics of insects: applications and quantitative genetic rationals / edited by JT Sorensen and R. Foottit. Amsterdam: Elsevier 1992: 95–112.

Rohlf FJ (2006) TpsRelw, relative warps analysis, Version 1.44. Department of Ecology and Evolution, State University of New York at Stony Brook.

Rohlf FJ (2008a) TpsUtil. Version 1.43. New York: Department of Ecology and Evolution, State University of New York at StonyBrook.

Rohlf FJ (2008b) TpsDig. Version 2.12; TpsRelw, Version 1.46. New York: Department of Ecology and Evolution, State University of New York at Stony Brook.

Rohlf FJ, Marcus LF (1993) A revolution in morphometrics. Trends in Ecology and Evolution 8: 129–132.

Roth LM (1970) Evolution and taxonomic significance of reproduction in Blattaria. Annual Review of Entomology 15: 75–96.

Sadeghi S, Adriaens D, Dumont HJ (2009) Geometric morphometric analysis of wing shape variation in ten European populations of *Calopteryx splendens* (Harris, 1782) (Zygoptera: Calopterygidae). Odonatologica 38(4): 341–357. https://natuurtijdschriften.nl/pub/592676

Schuh RT, Slater JA (1995) True Bugs of the World (Hemiptera: Heteroptera). Classification and Natural History. Cornell University Press, Ithaca, xii + 336 pp.

Sharp D, Muir F (1912) The comparative anatomy of the male genital tube in Coleoptera. Ecological Entomology 60(3): 477–642. https://doi.org/10.1111/j.1365-2311.1912.tb03107.x

Simmons LW (2014) Sexual selection and genital evolution. Austral Entomology 53 (1): 1–17. https://doi.org/10.1111/aen.12053

Simmons LW, Fitzpatrick JL (2016) Sperm competition and the coevolution of pre- and post-copulatory traits: weapons evolve faster than testes among onthophagine dung beetles. Evolution 70: 998–1008.

Sneath PH, Sokal RR (1973) Numerical taxonomy. The principles and practice of numerical classification. Department of Microbiology and Molecular Genetics, Michigan State University, USA.

Snodgrass RE (1957) A revised interpretation of the external reproductive organs of male insects. Smithsonian Miscellaneous Collections 135: 1–60.

Song H, Bucheli SR (2010) Comparison of phylogenetic signal between male genitalia and non-genital characters in insect systematics. Cladistics 26: 23–35.

Tuxen SL (1970) Taxonomist's glossary of genitalia in insects, second edn. Scandinavian University Press, Copenhagen.

Tüzün A (2009) Significance of wing morphometry in distinguishing some of the hymenoptera species. African Journal of Biotechnology 8(14): 3353–3363.

Villegas J, Feliciangeli MD, Dujardin JP (2002) Wing shape divergence between *Rhodnius prolixus* from Cojedes (Venezuela) and *Rhodnius robustus* from Mérida (Venezuela). Infection Genetics and Evolution 2(2): 121–128. https://doi.org/10.1016/S1567-1348(02)00095-3

Walker JA (2000) Ability of geometric morphometric methods to estimate a known covariance matrix. Systematic Biology 49: 686–696. https://doi.org/10.1080/106351500750049770

Waterhouse CO (1878) On the different forms occurring in the Coleopterous family Lycidae, with descriptions of new genera and species. Transactions of the Entomological Society London 26: 95–118.

West-Eberhard MJ (1983) Sexual selection, social competition, and speciation. The Quarterly Review of Biology 58(2): 155–183.

Xu HX, Kubáň V, Volkovitsch MG, Ge SQ, Bai M, Yang XK (2013) Morphological variability and taxonomy of *Coraebus hastanus* Gory & Laporte de Castelnau, 1839 (Coleoptera: Buprestidae: Agrilinae: Coraebini: Coraebina). Zootaxa 3682(1): 178–190. https://doi.org/10.11646/zootaxa.3682.1.9

Yoshizawa K, Johnson KP (2006) Morphology of male genitalia in lice and their relatives and phylogenetic implications. Systematic Entomology 31(2): 350–361. https://doi.org/10.1111/j.1365-3113.20-05.00323.x

Zelditch ML, Swiderski DL, Sheets HD, Fink WL. (2004) Geometric Morphometrics for Biologists: A Primer. Elsevier Academic Press. New York, 443 pp.

Zhao W, Liu HY, Ge XY, Yang YX (2023) Evaluating the significance of wing shapes in inferring phylogenetic proximity among the generic taxa: an example of Cantharinae (Coleoptera, Cantharidae). Arthropod Systematics & Phylogeny 81: 303–316. https://doi.org/10.3897/asp.81.e101411

Ziemert N, Jensen PR (2012) Phylogenetic approaches to natural product structure prediction. Methods in Enzymology 517: 161–182. https://doi.org/10.1016/B978-0-12-404634-4.00008-5

Zumpt F, Heinz HJ (1950) Studies on the sexual armature of Diptera II. A contribution to the study of the morphology and homology of the male terminalia of Calliphora and Sarcophaga. Entomologist's Monthly Magazine 86: 207–216.

Supplementary Material 1

Tables S1, S2

Author: Liu HY, Du RL, Zhao W, Yang XK, Yang YX (2023)
Data type: .pdf
Explanation note: Table S1. Eigen values and contributions of the principal components analysis of phallus shape in lateral view of the *Macrolycus dotatus* species group. — **Table S2.** Eigen values and contributions of the principal components analysis of phallus shape in ventral view of the *Macrolycus dotatus* species group.
Link: https://doi.org/10.3897/asp.81.e111281.suppl1

Supplementary Material 2

Figures S1–S4

Author: Liu HY, Du RL, Zhao W, Yang XK, Yang YX (2023)
Data type: .pdf
Explanation note: Figure S1. The principal component analysis of the phallus shapes in lateral view of the *Macrolycus dotatus* species group. — **Figure S2.** The principal component analysis of the phallus shapes in ventral view of the *Macrolycus dotatus* species group. — **Figure S3.** The canonical variates analysis of the phallus shapes in lateral view of the *Macrolycus dotatus* species group. — **Figure S4.** The canonical variates analysis of the phallus shapes in ventral view of the *Macrolycus dotatus* species group.
Link: https://doi.org/10.3897/asp.81.e111281.suppl2